Natural Hazards
https://doi.org/10.1007/s11069-018-3541-3

ORIGINAL PAPER

Damage assessment of the 2015 Mw 8.3 Illapel earthquake in the North-Central Chile

José Fernández[1] · César Pastén[1] · Sergio Ruiz[2] · Felipe Leyton[3]

Received: 27 May 2018 / Accepted: 19 November 2018

Abstract
Destructive megathrust earthquakes, such as the 2015 Mw 8.3 Illapel event, frequently affect Chile. In this study, we assess the damage of the 2015 Illapel Earthquake in the Coquimbo Region (North-Central Chile) using the MSK-64 macroseismic intensity scale, adapted to Chilean civil structures. We complement these observations with the analysis of strong motion records and geophysical data of 29 seismic stations, including average shear wave velocities in the upper 30 m, Vs_{30}, and horizontal-to-vertical spectral ratios. The calculated MSK intensities indicate that the damage was lower than expected for such megathrust earthquake, which can be attributable to the high Vs_{30} and the low predominant vibration periods of the sites. Nevertheless, few sites have shown systematic high intensities during comparable earthquakes most likely due to local site effects. The intensities of the 2015 Illapel earthquake are lower than the reported for the 1997 Mw 7.1 Punitaqui intraplate intermediate-depth earthquake, despite the larger magnitude of the recent event.

Keywords Subduction earthquake · H/V spectral ratio · Earthquake intensity

1 Introduction

On September 16, 2015, at 22:54:31 (UTC), the Mw 8.3 Illapel earthquake occurred in the Coquimbo Region, North-Central Chile. The epicenter was located at 71.74°W, 31.64°S and 23.3 km depth and the rupture reached an extent of 200 km × 100 km, with a near trench rupture that caused a local tsunami in the Chilean coast (Heidarzadeh et al. 2016; Li et al. 2016; Melgar et al. 2016; Ruiz et al. 2016; Tilmann et al. 2016). This event occurred near the northern end of the 1730 Mw ~ 9.0 megathrust earthquake rupture zone, which

Electronic supplementary material The online version of this article (https://doi.org/10.1007/s11069-018-3541-3) contains supplementary material, which is available to authorized users.

✉ César Pastén
cpasten@ing.uchile.cl

[1] Department of Civil Engineering, University of Chile, Av. Blanco Encalada 2002, Of. 431, 8370449 Santiago, Chile

[2] Department of Geophysics, University of Chile, Santiago, Chile

[3] National Seismological Center, University of Chile, Santiago, Chile

Published online: 26 November 2018

probably controls the seismic cycle of Central Chile (Carvajal et al. 2017; Dura et al. 2015; Udías et al. 2012). The 2015 Illapel earthquake seems to have a rupture similar to the previous 1880 and 1943 events (Fig. 1) (Beck et al. 1998; Ruiz and Madariaga 2018). However, the 1943 earthquake (Mw 7.9) was a smaller event than the 2015 one (Mw 8.3), as can be deduced from comparing seismograms of both events (Tilmann et al. 2016). Ruiz et al. (2016) proposed a possible connection between the 1997 Mw 7.1 intraplate, intermediate-depth Punitaqui earthquake (Lemoine et al. 2001; Pardo et al. 2002) with the 2015 megathrust earthquake due to an increase in the interplate seismicity after the 1997 event. Despite the reported observations of erosion and scouring in the coastal border, liquefaction of loose soil deposits, settlement in bridge abutments, rock falls in steep road slopes, and more than 7000 dwellings damaged (Candia et al. 2017; Minvu 2016), the 2015 Illapel earthquake produced limited damage in modern civil infrastructure in the Coquimbo Region. On the other hand, the localities of Monte Patria and Hurtado have repeatedly shown high levels of damage in past earthquakes, such as the 1943 Illapel and the 1997 Punitaqui earthquakes (Barrera 1943; Pardo et al. 2002), suggesting the influence of local site effects in their seismic response.

In order to elucidate site effects in the localities of the Coquimbo Region during the 2015 Illapel earthquake; firstly, we assessed the seismic damage using the MSK-64 intensity scale (Medvedev et al. 1964), which has been calibrated and used in previous Chilean earthquakes (Astroza et al. 2012; Monge and Astroza 1989). Then, we applied standard geophysical techniques, such as the single station horizontal-to-vertical spectral ratio (HVSR) of microtremor measurements and Vs_{30} measurements, for seismic site characterization. Given that the Coquimbo Region is instrumented with more than 29 strong motion sensors administered by the National Seismological Center (CSN), 16 of which registered the Illapel earthquake (stations and EW acceleration records are shown in Fig. 1), we also evaluated the horizontal-to-vertical response spectral ratio (HVRSR) using earthquake records. Finally, we integrated the results with the local surface geology.

2 Geological and seismological framework

The Coquimbo Region has two predominant morphologic units (Börgel 1983). First, the merge between the Andes and the Coastal Cordillera, characterized by E-W transverse mountain ranges, usually with heights from 600 to 1000 m above the sea level. This unit presents intense formation of valleys mainly associated with brooks and rivers erosion. The second unit consists of coastal plains of three types: marine, fluvial, and fluvial-marine. These plains reach a 30-km wide in the section between La Serena and Tongoy (Fig. 1) due to the mouth of rivers that deposit large amounts of materials, promoting the formation of continental dunes and beaches. Three large river basins, the Elqui, the Limarí, and the Choapa, generate fertile valleys filled with alluvial and colluvial quaternary deposits. In the coast, fossiliferous marine sedimentary rocks, of tertiary and quaternary age, merge with alluvial and wind terraced deposits of wide distribution (Bohnhorst 1967). The Coastal Cordillera mostly consists of Late Paleozoic and Mesozoic igneous rocks, whereas the Andes primary uplift dates to a Miocene event (Moreno and Gibbons 2007).

Several earthquakes have occurred in the subduction zone in front of the Coquimbo Region (North-Central Chile). Particularly, two of them caused important damage: the

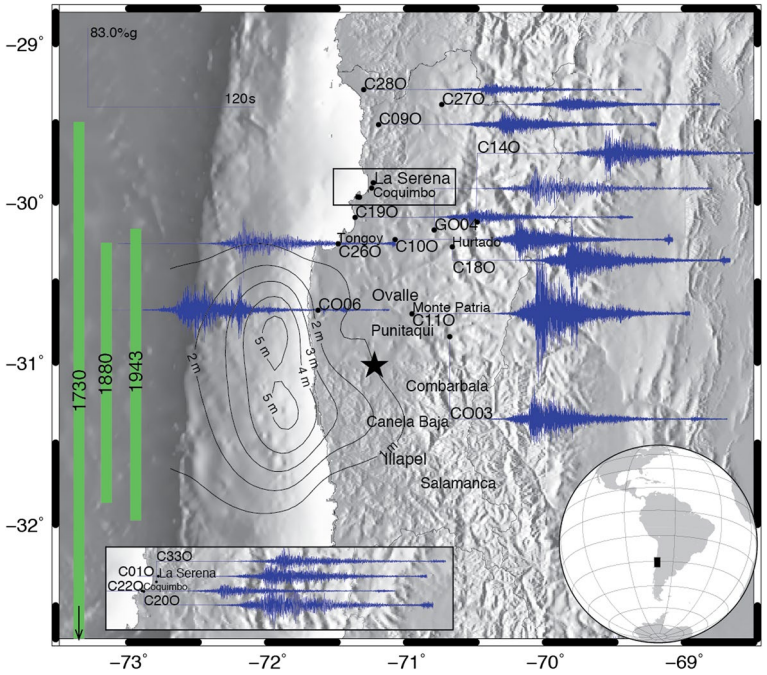

Fig. 1 North-Central Chile including the EW strong motion records of the 2015 Mw 8.3 Illapel Earthquake recorded by seismic stations of the National Seismological Center (CSN) Network. Iso-contour lines are the slip distribution of the Illapel 2015 earthquake (Ruiz et al. 2016) and the star is the epicenter of the 1997 Punitaqui earthquake. The green areas represent the 1730, 1880, and 1943 megathrust earthquakes approximate rupture area sizes

1943, Mw 7.9, Illapel interplate earthquake and the 1997, Mw 7.1, Punitaqui intraplate, intermediate-depth, earthquake. The 1943 Illapel earthquake produced a tsunami that reached 4–5 m of zero-to-crest wave high in the Coquimbo city shoreline (Beck et al. 1998) while Japan recorded a maximum wave high between 0.1 and 0.3 m (Hatori 1968). Local newspapers reported severe damage in infrastructure (Mercurio 1943; Norte 1943). The isoseismal map proposed by Greve (1946) defines the highest intensities in the cities of Ovalle, Combarbalá, Illapel, and Petorca (Figure S.1 in the Supplementary Material). This zone reached a maximum intensity of V (taken from an old I–VI intensity degree Chilean scale), which is equivalent to IX in the MSK intensity scale (Piñones 2002). However, Piñones (2002) performed a detailed analysis of ~ 20 masonry houses built in downtown Ovalle near 1925, their distribution within the neighborhood, and damage patterns from the 1943 Illapel earthquake, and concluded that the MSK intensities were not larger than VIII. On the other hand, the 1997 Punitaqui intraplate earthquake was felt with MSK intensities VI or larger from Salamanca in the south to Vicuña in the north of the Coquimbo Region (Pardo et al. 2002). There were 8 casualties, near 5000 destroyed houses, and other 15,700 houses damaged, besides soil and rock slope failures. Pardo et al. (2002) reported a maximum MSK intensity of IX near Punitaqui, which means over 50% of houses destroyed and the rest with several damage degrees. The MSK intensities of this intraplate intermediate-depth earthquake enable the comparison of the results with those obtained for the 2015 Illapel megathrust earthquake.

3 Damage assessment of the 2015 Illapel earthquake

The 2015 Illapel earthquake damaged mainly buildings while the tsunami destroyed structures along the coastline in the city of Coquimbo (Candia et al. 2017). The waves reached 4–5 m of maximum zero-to-crest high in the coast of the Coquimbo city; meanwhile, the tide recorded amplitudes of up to 78 cm in Japan (Heidarzadeh et al. 2016). There were 13 casualties and 6 missing people after the event (GEER 2015). The Chilean Ministry of Public Works (MOP in Spanish) reported eight damaged bridges, representing only 6.5% of all bridges in the Region; moreover, the damage to modern engineered infrastructure was limited. The settlement of bridge abutments and minor lateral spreading are the most common damage patterns. Liquefaction, landslides, and rockfalls were observed throughout the Region, mainly due to earthquake coseismic slip (Candia et al. 2017; GEER 2015).

The Chilean Ministry of Housing and Urban Development (MINVU in Spanish) provided the records of damaged dwellings used in this work. These data were collected in a survey developed within the following month to the main event (September 2015). The survey was part of a governmental program that allocated resources to rebuild the affected area. The sample consisted of 9317 dwellings in total, 7285 of which showed some degree of damage. They were classified according to 5 damage levels and the main construction materials were identified as adobe, masonry, wood, concrete, and other/undefined.

Figure 2 shows the results of the survey organized in counties. Adobe was the most affected material by the earthquake (37% of the total damaged dwellings) although a high percentage of other/undefined dwellings (31%) was reported, which could bias the analysis. Moreover, Fig. 2 shows that the Illapel and Canela counties had the largest number and the highest percentage of damaged dwellings, respectively. This result is expected due to the fact that they are the closest counties to the earthquake rupture (Fig. 1). On the other hand, the Monte Patria and the Hurtado counties show unexpectedly high damage, compared to their neighbor counties and considering that the distances to the earthquake rupture area are larger than the distances to the Illapel and the Canela counties (Fig. 1). Note

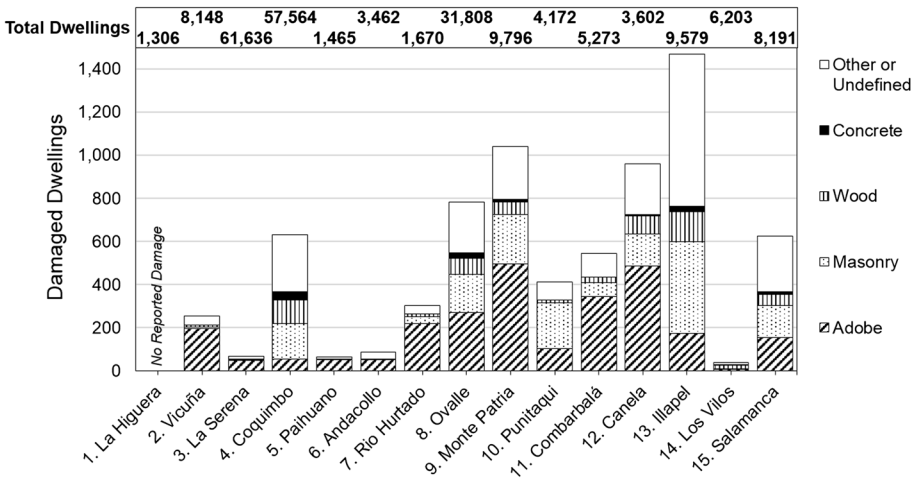

Fig. 2 Results of the Chilean Government survey after the 2015 Illapel earthquake. Number of damaged dwellings classified by construction material and counties, including the total number of dwellings in each county at the top of the chart

that, although the Coquimbo and the Ovalle counties show many damaged dwellings, they represent less than 2% of the total number of buildings in these counties.

4 MSK intensities

The methodology used to assess damage was the MSK-64 macroseismic intensity scale (Medvedev et al. 1964), adapted to Chilean conditions by Monge and Astroza (1989) and Díaz (2001). Briefly, the method consists in classifying buildings in one of three vulnerability classes: type A—adobe and brick masonry buildings, type B—unreinforced masonry buildings, and type C—reinforced and confined masonry buildings. The damage is classified in six grades, depending on the structural behavior during the earthquake: G0—No Damage, G1—Slight Damage, G2—Moderate Damage, G3—Heavy Damage, G4—Very Heavy Damage, and G5—Collapse or Destruction (Astroza et al. 2012). Then, based on field surveys after an earthquake, it is possible to generate a cumulative damage curve, which is compared with preset pattern curves defined by Monge and Astroza (1989). This method has been successfully applied in several Chilean earthquakes: the 1985 Valparaiso (Monge and Astroza 1989), the 1997 Punitaqui (Pardo et al. 2002), the 2007 Tocopilla (Astroza et al. 2008), and the 2010 Maule earthquakes (Astroza et al. 2012).

Díaz (2001) adapted the type A pattern curves for adobe in order to use an available government survey of damaged dwellings to estimate the 1997 Punitaqui earthquake MSK intensities. The survey, administered by the Chilean Ministry of Housing and Urban Development (MINVU), classified the damage in five grades instead of the six that the MSK-64 scale proposes. The grades defined by the MINVU (2016) are: D0—No damage, D1—Slight damage (non-structural damage), D2—Moderate damage (repairable damage greater than slight, habitability not compromised), D3—Repairable major damage (repairable structural damage, dwellers safety compromised), and D4—No repairable damage or actual to imminent collapse. The adapted pattern curves of cumulative damage are shown in Fig. 3 for intensities V–X as a function of the five damage grades (D0–D4).

Considering that adobe was the most damaged material during the 2015 earthquake (see Fig. 2) and that adobe is evenly distributed in the Coquimbo Region, according to the 2012 Population and Housing Chilean Census, we estimate the MSK intensities for adobe

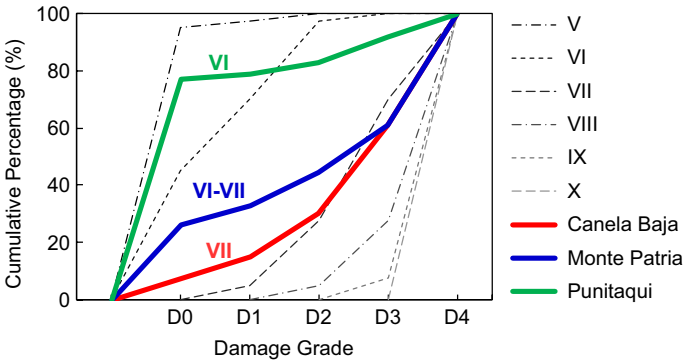

Fig. 3 Evaluation of MSK intensity by comparison with the pattern curves (gray dashed lines) defined by Díaz (2001). Direct graphic application of the method in the localities of Canela Baja, Monte Patria, and Punitaqui is shown in colors

buildings (A-type of buildings in MSK definition) using the pattern curves proposed by Díaz (2001) and the damage evaluation survey performed by the MINVU after the Illapel Earthquake.

The cumulative damage curve was calculated by dividing the number of damaged adobe buildings in the total number of buildings in a given area (village, town or city). The total building stock in the region was estimated from the 2012 Population and Housing Chilean Census. The intensity degree was determined by comparing the cumulative damage curve with the pattern curve immediately above. The half degree is determined by areas interpolation method (Menéndez 1991), that uses the ratio between the areas above and below the measured curve limited by the pattern curves. Figure 3 shows examples of cumulative damage curves for three localities: Canela Baja, Monte Patria, and Punitaqui.

Figure 4a shows the calculated MSK intensities of the 2015 Illapel earthquake; the number of damaged dwellings and MSK intensities for each locality are shown in Table 1 (details of the damage grades used in the calculations are shown in Table S.1 in the Supplementary Material). Figure 4b shows the MSK intensities of the 1997 Punitaqui earthquake (Díaz 2001). This figure allows identifying some factors that influence the intensity distribution. In the first place, the location of the earthquake source defines the general intensity distribution, as near-source localities exhibit higher intensities compared to the most distant ones. Monte Patria and Hurtado are exceptions due to the fact that they show large MSK intensities compared to the neighbor localities and given the distance to the earthquake rupture area. These apparent anomalies could be produced by local amplification be due to local site conditions.

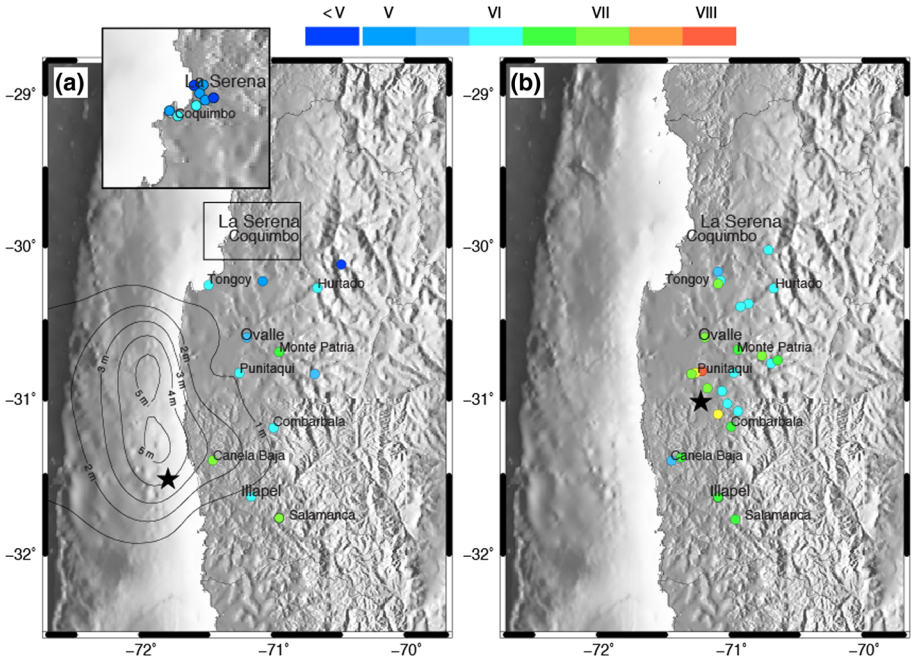

Fig. 4 MSK intensities distribution maps at locality level. **a** MSK intensities calculated in this study for the 2015 Illapel megathrust earthquake. **b** MSK intensities reported by Díaz (2001) for the 1997 Punitaqui intraplate intermediate-depth earthquake. The stars represent the epicenters of the events

Table 1 Seismic site characterization for each processed station

Station		Predominant period (s)			PGA (g)	Vs_{30} (m/s)	I_{MSK}		Surface geology
Code	Locality	T_P	T_{PS}	T_{PE}			1997	2015	
C01O	La Compañía Alta, La Serena	0.77	0.81	0.94	0.16	450	V	V	Terraced marine sediments: sandstones, calcarenites, coquinas and conglomerates, usually with a thin quaternary surface (Tec-Qal)
C04O	La Pampa, La Serena	1.17	1.27	–	–	475	V	VI	
C05O	Punitaqui	Flat	0.09*	–	–	–	VII–VIII	VI	Tertiary continental sediments over Jurassic granite (Qc-Kg)
C06O	La Florida, La Serena (Airport)	–	Flat	–	–	–	V	V	Atacama gravels, poorly consolidated, including terraced river deposits (Tega)
C07O	Illapel	0.17	0.21	–	–	655	VI–VII	VI	Alluvial and colluvial sediments over conglomerates, sandstones, breccia and limolites (Qac-Tc; Ki1)
C08O	Combarbalá	1.63	–	–	–	827	VI–VII	VI	Sedimentary and continental volcanic sequences, with marine intercalations (Ki2c).
C09O	La Higuera	0.19	0.18	0.18	0.19	750	V–VI	–	Atacama gravels, poorly consolidated, including terraced river deposits (Tega-Qal; Kg)
C10O	Andacollo	–	0.16**	0.19	0.30	–	VI	V	Quaternary continental sediments from clastic continental sedimentary and volcanic andesitic rocks (Qc-Kqm)
C11O	Monte Patria	0.29	0.34	0.34	0.77	625	VI–VII	VI–VII	Quaternary alluvial deposits surrounding by volcanic rocks (Qal-Kv)
C12O	Canela Baja	0.08	0.08*	–	–	–	V–VI	VII	Continental sediments cutting across intrusive (granodiorites and tonalites) (Qc-Jmi4).
C13O	Cerrillos, Limarí	0.45	0.52	–	–	500	VI–VII	–	Quaternary alluvial deposits and continental sediments (Qal-Qc)
C14O	Pisco Elqui	–	0.58	0.66	0.23	–	VI	V	Quaternary alluvial and colluvial sediments over tonalites, quartz diorites of coarse grain with hornblende and biotite (Qac-Cg)
C15O	El Trapiche	–	0.13*	–	–	–	–	–	Quaternary alluvial deposits over tertiary granite and granodiorite (Qal-Kgd)
C16O	La Compañía, La Serena	0.77	0.78*	–	–	280	V	–	Wind and alluvial quaternary deposits (Qe-Qal)

Table 1 (continued)

Station		Predominant period (s)			PGA (g)	Vs_{30} (m/s)	I_{MSK}		Surface geology
Code	Locality	T_P	T_{PS}	T_{PE}			1997	2015	
C18O	Hurtado	–	0.18	0.20	0.49	–	VI–VII	VI	Alluvial and colluvial sediments over the joint of rhyolitic and andesitic breccia and tuffs, with granodiorites and monzogranites (Qac; Tc-Tle)
C19O	La Herradura	Flat	Flat	Flat	0.11	1100	–	V	Andesitic volcanic rocks, including breccia and tuff (rhyolitic) (Kt)
C20O	Buen Pastor, Coquimbo (Hospital)	0.85	0.90	0.97	0.25	740	V	V	Terraced marine sediments: sandstones, calcarenites, coquinas and conglomerates, usually with a thin quaternary surface (Tec-Qal)
C22O	Buen Pastor, Coquimbo (UCN)	Flat	Flat	Flat	0.10	1230	V	V	Jurassic granite (JKg)
C23O	Salamanca	0.45	–	–	–		VI–VII	VII	Alluvial and colluvial sediments with granodiorites (Qac; Ki1)
C26O	Tongoy	0.59	0.69	0.81	0.29	380	VI–VII	VI	Continental volcanic andesitic and sedimentary rocks (Ja-Qal)
C27O	Tres Cruces	–	Flat	Flat	0.11	–	–	–	High Andes tertiary granodiorite (Tgd)
C28O	Los Choros	–	0.22	0.30	0.09	–	–	–	Quaternary alluvial over wind deposits and tertiary terraced marine sediments (Qal-Qe; Tec)
C29O	Ovalle	1.10	–	–	–	799	VII	V–VI	Quaternary fluvial deposits: gravels, sands, and limes deposited by actual rives (Qf)
C33O	Las Vegas, La Serena (Stadium)	0.34	0.36	0.36	0.12	590	V	VI	Quaternary alluvial deposits over terraced marine sediments (Qal-Tec)
CO02	Ciudad Oriente, Combarbalá	0.25	0.25	–	–	400	–	–	Hydrothermal alteration (combarbalite) (ah)
CO03	Pedregal	Flat	Flat	Flat	0.32	700	VI–VII	–	Alluvial and colluvial sediments, valley-filling deposits, surrounding by andesitic lavas and breccia (Qac-Kv)
CO05	Universidad, La Serena	Flat	Flat	–	–	775	V	V	Atacama gravels, poorly consolidated, including terraced river deposits (Tega)
CO06	Fray Jorge	0.24**	0.21**	0.21	0.35	–	–	–	Jurassic granite to granodiorite, gneiss diorite (Jgd-Jdn)

Table 1 (continued)

Station		Predominant period (s)			PGA (g)	Vs_{30} (m/s)	I_{MSK}		Surface geology
Code	Locality	T_P	T_{PS}	T_{PE}			1997	2015	
GO04	Algodones (Cerro Tololo)	0.50	0.66	0.99	0.29	–	–	–	Basaltic and rhyolitic andesitic volcanic rocks, interspersed with sedimentary rocks (Kle-Kv)

T_P, predominant period from microtremor HVSR; T_{PE}, predominant period from the 2015 Illapel earthquake HVRSR; T_{PS}, predominant period from the mean curve of earthquake data HVRSR; Flat, HVSR or HVRSR amplitude lower than 2

*Few earthquake records

**Peaks with low amplitude ($2 \leq$ HVRSR-HVSR ≤ 3)

– Data not available

5 Seismic site characterization

In order to analyze the seismic response of the Coquimbo Region sites, we used the Horizontal-to-Vertical Response Spectral Ratio (HVRSR), applied to earthquake records in single stations (Idini et al. 2017; Zhao et al. 2006), as well as the Horizontal-to-Vertical Spectral Ratio (HVSR) of microtremor measurements (Nakamura 1989).

Local earthquake data were obtained from the Chilean seismological network in 29 stations of the Coquimbo Region, administered by the National Seismological Center (CSN). We considered 891 strong motion records, from accelerometers, corresponding to 130 Mw > 5.0 earthquakes with hypocenters in the Coquimbo Region, listed in Table S.2 in the Supplementary Material; on the other hand, microtremor data were obtained from (Leyton et al. 2018).

To calculate HVRSR curves from earthquakes records, we followed Idini et al. (2017). First, acceleration records in each component are cut between 5 and 95% of the cumulative Arias Intensity. Then, a Butterworth filter is applied from 0.2 to 25 Hz and the 5%-damped acceleration response spectra are calculated for each component. Finally, the horizontal components are combined by the geometric mean and divided by the response spectrum of the vertical component.

Microtremor measurements are processed using the H/V application of the Geopsy® software. We selected 30 s time windows for the spectral analysis and used the Konno and Ohmachi (1998) filter with a smoothing constant $b = 40$. Figure 5 shows the results of the HVRSR of earthquake records and the HVSR of microtremors in each station. The figure highlights the HVRSR curve for the Illapel 2015 mainshock, the mean curve for the earthquake data, and the number of earthquake records considered in each station.

Table 1 summarizes the predominant periods of the stations estimated from the HVRSR of the mean curve for the earthquake data (T_{PS}) and the 2015 Illapel earthquake (T_{PE}), as well as the predominant period from microtremor HVSR (T_P). Available Vs_{30} and local surface geology was also included to complete the characterization. The surface geology was collected from Chilean Geological Charts (Aguirre and Egert 1970; Bohnhorst 1967; Moscoso et al. 1982; Mpodozis and Cornejo 1988; Rivano and Sepúlveda 1991), whereas Vs_{30} values were taken from the geophysical characterization of Chilean seismological network performed by Leyton et al. (2018).

Predominant periods in most sites are consistent with the surface geology composed by thin layers (< 50 m) of alluvial or colluvial sedimentary quaternary deposits over Paleozoic to quaternary bedrock. Based on the HVRSR predominant periods, 20 out of the 29 studied stations are classified as s_{III} ($T_{PS} < 0.4$ s) or better, according to the Idini et al. (2017) classification. Moreover, 16 of 17 stations with available Vs_{30} are classified as C class (dense or firm soil, $Vs_{30} \geq 350$ m/s) or better according to Chilean Seismic Code (MINVU 2011).

From the predominant periods and peak amplitudes of the curves in Fig. 5, we built Fig. 6, which confirms a good correlation between the periods determined from earthquake data (HVRSR) and microtremor measurements (HVSR). This correlation is partially extended to peak amplitudes (Fig. 6b): the mean curve for the earthquake data (Fig. 5) is strongly correlated with the curve obtained from microtremors, while amplitudes from the 2015 Illapel earthquake largely differ from those of microtremors. Thus, we could use HVSR from microtremors as well as HVRSR from seismic records in order to determine the predominant period of the sites; however, amplitudes from a single large event record may not be representative of the sites.

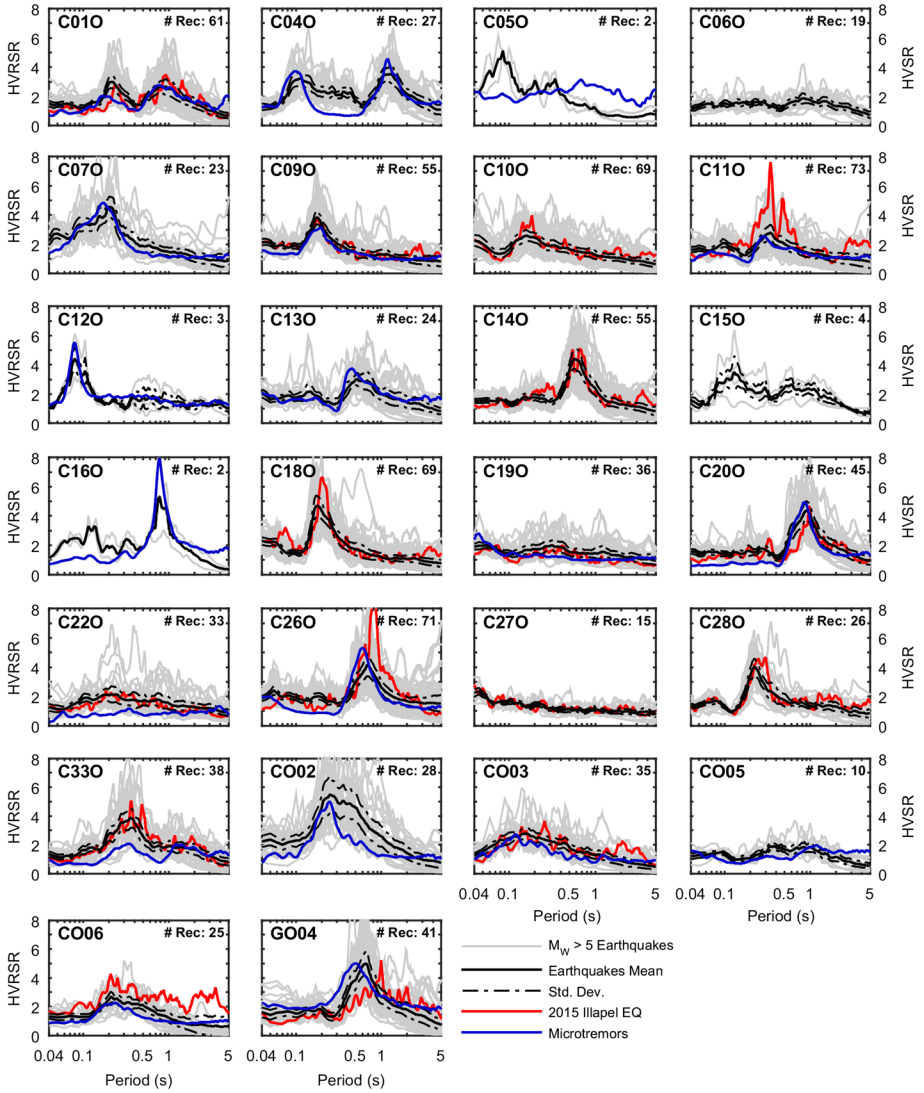

Fig. 5 Results of HVSRS calculated from strong ground-motion records and HVSR from microtremor measurements at the seismological stations in the Coquimbo Region. Each plot indicates the number of recorded earthquakes in the station (# Rec)

6 Discussion

From the MSK intensities shown in Fig. 4, we infer that the 1997 Punitaqui earthquake was more destructive than the 2015 Illapel earthquake, probably due to the shorter and more direct path of seismic waves from the source to the surface, despite its lower magnitude and associated seismic energy (Figure S.2 in the Supplementary Material shows the attenuation of MSK intensities with the hypocentral distance for both earthquakes).

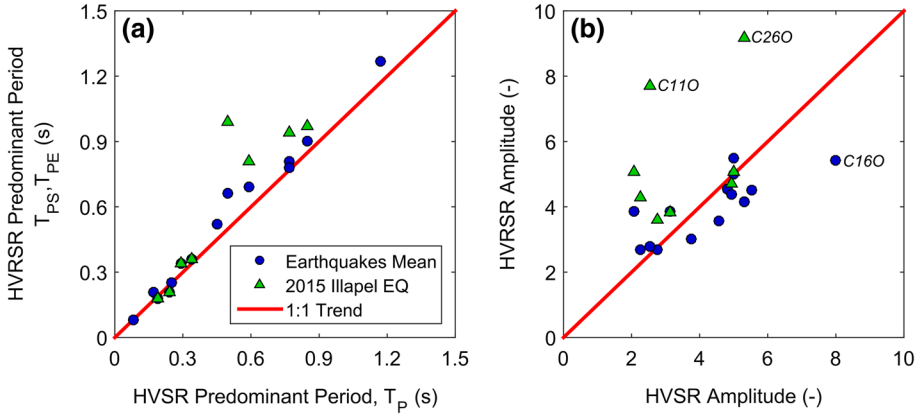

Fig. 6 Comparison between earthquakes HVRSR and microtremors HVSR. **a** Predominant periods and **b** amplitudes at predominant periods. Blue dots are computed from the mean curve of earthquake data, whereas green triangles are calculated from the records of the 2015 Illapel earthquake

Figure 7 shows the horizontal peak ground acceleration (PGA) recorded in the seismic stations during the 2015 Illapel earthquake as a function of the distance to the earthquake rupture area. Unfortunately, the closest stations to the earthquake rupture did not record the main event; hence, the shortest reported distance is 33 km (station CO06). The ground-motion prediction equation proposed by Idini et al. (2017) for stiff soils (class s_I: non-identifiable predominant period and HVRSR amplitude ≤ 2) is included as a reference. Most of the PGA values follow the attenuation trend with the distance to the rupture; however, stations C11O (Monte Patria) and C18O (Hurtado) recorded unexpectedly very high PGA.

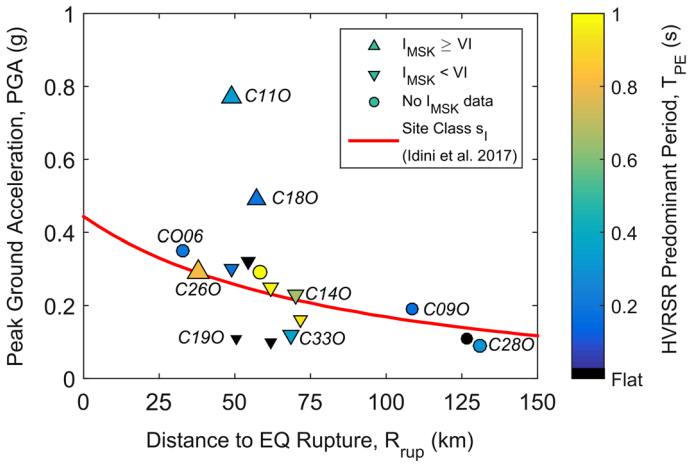

Fig. 7 Peak ground acceleration (PGA) as a function of the distance to the rupture of the 2015 Illapel earthquake. The results are compared with the Idini et al. (2017) ground-motion prediction equation for reference rock site (s_I). The color of the symbols is associated with the predominant periods from the 2015 Illapel earthquake HVRSR curves and the size of the symbol is proportional to the peak amplitude

The percentages of damaged dwellings in Monte Patria (11%) and Hurtado (18%) counties are comparable to those in Illapel (15%) and Canela (27%), even though their distances to the earthquake rupture are larger. The damage is consistent with the high MSK intensities calculated in this study and the low predominant periods of the soil that may resonate with the one- and two-story buildings in the area. However, it is desirable to revise the MSK methodology in adobe, because dwellings built on this material have low natural vibration periods, similar to the predominant periods of soils in the zone; hence, this kind of analysis could be misleading due to resonance phenomenon. Figure 7 also shows that the highest MSK intensities are related to the largest peaks amplitudes from the 2015 Illapel earthquake HVRSR curves (Fig. 5), independent of the associated predominant period. From the results shown in Fig. 7, we propose that moderate-to-large earthquakes, with important high-frequency energy content, could induce high intensities and damage in soils with low predominant period (e.g., C110 and C180 sites) and rigid structures, such as adobe houses.

7 Conclusions

Calculated MSK intensities indicate that the damage was lower than expected for the 2015 Mw 8.3 Illapel megathrust earthquake. We propose that the computed low MKS values are mainly controlled by the rigid soils where localities are placed in the North-Central zone of Chile. Despite the high Vs_{30} values and the short predominant periods of sites, some localities evidenced more damage. In those closest to epicenter, the damage could be explained as a combination of higher radiation energy from the earthquake rupture and the coupled vibration of stiff soils and stiff adobe structures. On the other hand, local amplification effects could explain the damage in the farther localities, such as Monte Patria and Hurtado, which have shown sustained high damage levels in past earthquakes. The predominant periods and Vs_{30} in these two sites are not particularly different compared to other stations, so site effects could not be directly attributable to soil amplification, and topographic effects may contribute. In addition, PGA seems to be a good predictor of damage in the analyzed sites.

The 1943 Illapel and the 2015 Illapel thrust earthquakes are seismogenically similar, developed comparable tsunamis, and produced equivalent damage to civil infrastructure. However, both earthquakes caused lower damage than the evidenced in the 1997 Punitaqui intraplate intermediate-depth earthquake. Limited information about the 1943 Illapel earthquake do not allow a definitive conclusion; nevertheless, MSK intensities data indicate that the 1997 Punitaqui is indeed a more destructive event than the 1943 and 2015 Illapel earthquakes, despite its smaller magnitude.

Spectral ratios calculated from earthquakes and microtremors are consistent even when slight shifts in the predominant periods are detected, which can be related to a stiffness degradation induced by the earthquake. Thus, microtremor HVSR technique works well to predict soils predominant periods in the Coquimbo Region. Geological information of each station is consistent with observed behavior in HVRSR and HVSR curves, as well as Vs_{30} values, where predominant periods represent stiff soil deposits and rock outcrops, as expected.

Acknowledgements This study was partially supported by a FONDECYT N° 1170430 and by PRS (Programa Riesgo Sísmico of Universidad de Chile). C. Pastén thanks the support from the Advanced Mining Technology Center (AMTC FB0809 PIA CONICYT). Data were freely retrieved from the Chilean Strong

Motion Database, operated by the National Seismological Center (evtdb.csn.uchile.cl, last accessed May 2017).

References

Aguirre L, Egert E (1970) Geología del Cuadrángulo Lambert (La Serena), Región de Coquimbo, Chile (1:50,000), Carta Geológica No. 23. Instituto de Investigaciones Geológicas de Chile

Astroza M, Omerovic J, Astroza R, Music J, Saragoni R, Alvarez I, Covarrubias A, Morales E, Vladilo S, Rabello O (2008) Intensity and damage assessment of the 2007 tocopilla earthquake, Chile. Earthquake Engineering and Research Institute, Oakland

Astroza M, Ruiz S, Astroza R (2012) Damage assessment and seismic intensity analysis of the 2010 (Mw 8.8) Maule earthquake. Earthq Spectra 28(S1):S145–S164

Barrera (1943) El Gobierno adopta rápidas medidas de auxilio para los damnificados del Norte. El Mercurio

Beck S, Barrientos S, Kausel E, Reyes M (1998) Source characteristics of historic earthquakes along the Central Chile subduction zone. J S Am Earth Sci 11(2):115–129

Bohnhorst HT (1967) Geología de la hoja Ovalle: Provincia de Coquimbo, Boletín No. 23. Instituto de Investigaciones Geológicas de Chile, Santiago

Börgel R (1983) Geografía de Chile, Tomo II, Geomorfología. Instituto Geográfico Militar, Santiago

Candia G, de Pascale G, Montalva G, Ledezma C (2017) Geotechnical aspects of the 2015 Mw 8.3 Illapel megathrust earthquake sequence in Chile. Earthq Spectra 33(2):709–728

Carvajal M, Cisternas M, Catalan P (2017) Source of the 1730 Chilean earthquake from historical records: implications for the future tsunami hazard on the coast of Metropolitan Chile. J Geophys Res Solid Earth 122(5):3648–3660

Díaz O (2001) Estudio de los efectos de las condiciones locales en el terremoto de Punitaqui 1997. Memoria para optar al título de Ingeniero Civil. Universidad de Chile, Santiago

Dura T, Cisternas M, Horton B, Ely L, Nelson A, Wesson R, Pilarczyk J (2015) Coastal evidence for Holocene subduction-zone earthquakes and tsunamis in Central Chile. Quart Sci Rev 113:93–111

GEER (2015) Geotechnical reconnaissance of the 2015 Mw 8.3 Illapel, Chile earthquake. Report No. GEER-043, Geotechnical Extreme Events Reconnaissance Association

Greve F (1946) Descripción de los principales efectos y ubicación del epicentro de los sismos destructores sentidos en Chile en los años 1942-43-44-45 y 46. Instituto Sismológico, Universidad de Chile, Santiago

Hatori T (1968) Study on distant tsunamis along the coast of Japan. Part 2: Tsunamis of South America origin. Bull Earthq Res Inst 46(15):345–359

Heidarzadeh M, Murotani S, Satake K, Ishibe T, Gusman AR (2016) Source model of the 16 September 2015 Illapel, Chile, Mw 8.4 earthquake based on teleseismic and tsunami data. Geophys Res Lett 43(2):643–650

Idini B, Rojas F, Ruiz S, Pastén C (2017) Ground motion prediction equations for the Chilean subduction zone. Bull Earthq Eng 15(5):1853–1880

Konno K, Ohmachi T (1998) Ground-motion characteristics estimated form spectral ratio between horizontal and vertical components of microtremor. Bull Seismol Soc Am 88(1):228–241

Lemoine A, Madariaga R, Campos J (2001) Evidence for eathquake interaction in Central Chile: the July 1997–September 1998 sequence. Geophys Res Lett 28(14):2743–2746

Leyton F, Leopold A, Hurtado G, Pasten C, Ruiz S, Montalva G, Saez E (2018) Geophysical characterization of the Chilean seismological stations: first results. Seismol Res Lett 89(2A):519–525

Li L, Lay T, Cheung KF, Ye L (2016) Joint modeling of teleseismic and tsunami wave observations to constrain the 16 September 2015 Illapel, Chile, Mw 8.3 earthquake rupture process. Geophys Res Lett 43(9):4303–4312

Medvedev S, Sponheuer W, Karník V (1964) Neue seismische Skala Intensity scale of earthquakes, 7. Tagung der Europäischen Seismologischen Kommission vom 24.9. bis 30.9. 1962. Jena, Veröff. Institut für Bodendynamik und Erdbebenforschung in Jena, Deutsche Akademie der Wissenschaften zu Berlin, pp 69–76

Melgar D, Fan W, Riquelme S, Geng J, Liang C, Fuentes M, Vargas G, Allen RM, Shearer PM, Fielding EJ (2016) Slip segmentation and slow rupture to the trench during the 2015, Mw8.3 Illapel, Chile earthquake. Geophys Res Lett 43(3):961–966

Menéndez P (1991) Atenuación de las Intensidades del Sismo del 3 de marzo de 1985 en función de la Distancia a la Zona de Ruptura y del Tipo de Suelo. Memoria para optar al Título de Ingeniero Civil. Universidad de Chile, Santiago

Mercurio E (1943) La Provincia de Coquimbo fue la más afectada por el temblor de ayer. El Mercurio

MINVU (2011) Aprueba Reglamento que Fija el Diseño Sísmico de Edificios y Deroga Decreto No. 117, de 2010, Decreto Supremo 61 del Ministerio de Vivienda y Urbanismo, 2 November 2011. Gobierno de Chile

Minvu (2016) Plan de Reconstrucción Región de Coquimbo 2015. http://www.minvu.cl/opensite_20151002093225.aspx. 15 March 2017

Monge J, Astroza M (1989) Metodología para determinar el grado de Intensidad a partir de los daños. 5as Jornadas Chilenas de Sismología e Ingeniería Antisísmica ACHISINA, 7–11 Agosto 1989, Santiago, Chile, pp 483–492

Moreno T, Gibbons W (2007) The geology of Chile. The Geological Society, London

Moscoso R, Nasi C, Salinas P (1982) Geología de la Hoja Vallenar y parte Norte de La Serena, Regiones de Atacama y Coquimbo, Chile (1:250,000), Carta Geológica No. 55. Servicio Nacional de Geología y Minería

Mpodozis C, Cornejo P (1988) Geología de la Hoja de Pisco Elqui, Región de Coquimbo (1:250,000), Carta Geológica No. 68. Servicio Nacional de Geología y Minería

Nakamura Y (1989) A method for dynamic characteristics estimation of subsurface using microtremor on the ground surface. QR Railw Tech Res Inst 30(1):25–33

Norte E (1943) Un violento temblor azotó ayer la Provincia de Coquimbo. El Norte

Pardo M, Comte D, Monfret T, Boroschek R, Astroza M (2002) The October 15, 1997 Punitaqui earthquake (Mw = 7.1): a destructive event within the subducting Nazca plate in central Chile. Tectonophysics 345(1–4):199–210

Piñones A (2002) Efectos del Sismo del 14 de octubre de 1997 en la Ciudad de Ovalle. Memoria para optar al Título de Ingeniero Civil. Universidad de Chile, Santiago

Rivano S, Sepúlveda P (1991) Geología de la Hoja de Illapel, Región de Coquimbo, Chile (1:250,000), Carta Geológica No. 69. Servicio Nacional de Geología y Minería

Ruiz S, Madariaga R (2018) Historical and recent large megathrust earthquakes in Chile. Tectonophysics 733:37–56

Ruiz S, Klein E, del Campo F, Rivera E, Poli P, Metois M, Christophe V, Baez JC, Vargas G, Leyton F (2016) The seismic sequence of the 16 September 2015 Mw 8.3 Illapel, Chile, earthquake. Seismol Res Lett 87(4):789–799

Tilmann F, Zhang Y, Moreno M, Saul J, Eckelmann F, Palo M, Deng Z, Babeyko A, Chen K, Baez J (2016) The 2015 Illapel earthquake, central Chile: a type case for a characteristic earthquake? Geophys Res Lett 43(2):574–583

Udías A, Madariaga R, Buforn E, Muñoz D, Ros M (2012) The large Chilean historical earthquakes of 1647, 1657, 1730, and 1751 from contemporary documents. Bull Seismol Soc Am 102(4):1639–1653

Zhao JX, Irikura K, Zhang J, Fukushima Y, Somerville PG, Asano A, Ohno Y, Oouchi T, Takahashi T, Ogawa H (2006) An empirical site-classification method for strong-motion stations in Japan using H/V response spectral ratio. Bull Seismol Soc Am 96(3):914–925